ELSEVIER

Chemical Engineering Journal 121 (2006) 9–16

Chemical Engineering Journal

www.elsevier.com/locate/cej

Synthesis of CdS nanocrystals and Au/CdS nanocomposites through ultrasound activation liquid–liquid two-phase approach at room temperature

Dunliang Jian, Qiuming Gao *

State Key Laboratory of High Performance Ceramics and Superfine Microstructure, Graduate School, Shanghai Institute of Ceramics, Chinese Academy of Sciences, Shanghai 200050, PR China

Received 13 February 2006; received in revised form 24 April 2006; accepted 26 April 2006

Abstract

CdS nanocrystals were prepared and further 50 times scale-up syntheses were carried out through a novel ultrasound activation liquid–liquid (water and cyclohexane) two-phase approach at room temperature for the first time. Further preparation of Au/CdS nanocomposites were also realized by the same method. This fast, energy saving, environmentally benign, high-yield approach will benefit greatly to both fundamental mechanism research and industrial utilization development.

PACS: 81.07.-b; 81.16.-c; 81.05.Bx; 81.05.Dz

Keywords: Ultrasound activation liquid–liquid two-phase approach at room temperature; CdS nanocrystals; Au/CdS nanocomposites

1. Introduction

Semiconductor nanocrystals are of great interests for both fundamental research and industrial development because of their exciting utilization in the fields of light-emitting diode, electroluminescent device, laser, hydrogen producing catalyst, biological label and immune diagnosis [1–17]. They were usually prepared in the liquid reaction system at high temperature for several hours. Those methods are either expensive, explosive, moisture sensitive or extreme dangerous, toxic or energy consuming, thus difficult to satisfy the need of industry. For example, most of the methods for preparation of chalcogenide nanocrystal quantum dots required dangerous high temperature liquid system (typically 573 K) using air and temperature sensitive organometallic precursors such as $Cd(CH_3)_2$, $Zn(C_2H_5)_2$ or environmental pollution agents such as H_2S, toluene and/or organophosphorous compounds. Therefore, developing novel facile preparation methods under mild conditions using "green" agents is still of challenge for both industry and academia [18–21]. Recently, much attention was paid to develop liquid–liquid approach for synthesizing nanocrystal metals and metal oxides [22–27]. To the best of our knowledge, there was no report on the synthesis of semiconductor chalcogenide nanocrystal quantum dots under this approach up to now [21,28,29]. Ultrasonic-involved process in synthetic chemistry is a fast-growing research area due to the advantage of rapidly efficient reaction under mild condition. Besides, in contrast to traditional chemical process smaller size particles could form under ultrasonic condition [30–33]. The effects of ultrasound result from acoustic cavitations, e.g., the formation, growth and implosive collapse of bubbles in liquid. The implosive collapse of the bubbles can generate localized hotspot through adiabatic compression to produce teeny local instantaneous high temperature (estimated 5000 K in water) and high pressure (over 1800 kPa in water), which may activate many chemical precursors to react under apparently mild conditions. In this paper, we reported the preparation of the CdS semiconductor nanocrystal quantum dots through combining both ultrasound activation and liquid–liquid two-phase approach.

Recently, various researches on heterogeneous nanostructure with multifunction were carried out [34]. Metal/semiconductor composites are of most interest because of their modified electronic structures and properties [35–38,39–48]. Besides, the composites of metal/chalcogenide Co/CdSe or

* Corresponding author. Tel.: +86 21 52412513; fax: +86 21 52413122.
E-mail address: qmgao@mail.sic.ac.cn (Q. Gao).

1385-8947/$ – see front matter © 2006 Elsevier B.V. All rights reserved.
doi:10.1016/j.cej.2006.04.012

alloy/chalcogenide FePt/CdS demonstrated bifunctions of magnets and semiconductors [43,44]. Further preparation and characterization of the related nanocomposites should be developed. Herein, the Au/CdS nanocomposites with the bifunctions of heavy metal "tracer" and semiconductors were prepared through the above ultrasound activation liquid–liquid two-phase approach.

2. Experimental

2.1. Preparation of CdS nanoparticles

All experiments were carried out at room temperature around 303 K (between 298 and 305 K) and the chemicals used were analytical grade except for special claim. First, 135 mg of octadecyl amine was dispersed in 10 mL of cyclohexane in a 25 mL beaker. Then, 3.2 mg of sulfur (0.1 mmol) was added under ultrasonic action for 5 min with the beaker sealed by polyethylene film and a colorless transparent organic solution formed. And then, 26.7 mg of cadmium acetate (0.1 mmol) was added and dissolved, following by the addition of 5.0 mL of sodium borohydride (25 mM) aqueous solution. The beaker with the reaction mixture was put in an ultrasonic recipient (ultrasonic instrument SK3300HP, 160 W, 59 kHz) for a certain time. The ultrasound process may result in an increase of temperature less than 5 K. The reaction system can be quenched by withdrawing the beaker from ultrasonic container, settling for half a minute and decanting organic phase. UV–vis absorption spectra were used to determine the aliquots at different ultrasonic activation reaction time. When the reaction was quenched in 2 min, the organic phase displayed pale green; when quenched in 10 min, the organic phase turned into pale green yellow, which was kept even if the reaction was prolonged to 6 days without obvious absorption peak shift in the UV–vis spectra. Typically, when the reaction finished in 15 min, the product was got by centrifugation (9000 rpm) from the organic phase, in which an additional 20 mL of ethanol was added. The product was re-dispersed in cyclohexane solvent and re-precipitated with ethanol to purify the nanoparticles. Parts of the nanoparticles were re-dispersed in cyclohexane forming organic colloids which were preserved in refrigerator (277 K). Both solid powders and organic colloids were used for the further characterization.

2.2. Scale-up synthesis of CdS nanoparticles

For scale-up synthesis, 50 times of the related cadmium acetate and sulfur reactants were chosen. The reaction was still carried out in an ultrasonic recipient. In a typical scale-up synthesis, 6.75 g (25 mmol) of dodecyl amine was dispersed in 100 mL of cyclohexane in a 200 mL beaker. After adding 160 mg of sulfur (5 mmol) which was dispersed under ultrasonic action for 5 min, the colorless transparent organic phase formed. Then, 1.33 g of cadmium acetate (5 mmol) was dispersed and 20 mL of sodium borohydride (250 mM) solution was added. The purification was similar to that of the above procedure. The yield of CdS nanoparticles was about 90%.

2.3. Synthesis of Au/CdS bifunctional nanocomposites

As to preparation of the Au/CdS bifunctional nanocomposites, gold nanoparticles were synthesized firstly using chloroauric acid as the Au sources. First, 135 mg of octadecyl amine was dispersed in 10 mL of cyclohexane in a 25 mL beaker and a colorless transparent organic solution formed. Then, 4.0 mL of chloroaurum acid (25 mM) aqueous solution was added and an orange organic phase formed along with a colorless or somewhat white aqueous phase. After the injection of 10 mL of sodium borohydride (25 mM) aqueous solution, the liquid–liquid two-phase reaction mixture was put into an ultrasonic recipient. The organic phase changed to rosered in 30 s and the beautifully rosered Au sols were got after separation of the colorless aqueous phase. The purification was similar to that of the above procedure and the rosered Au nanoparticles were allowed to disperse in cyclohexane.

A 135 mg of dodecyl amine and 3.2 mg of sulfur (0.1 mmol) were added into the above rosered Au cyclohexane mixture and the whole mixture was put in an ultrasonic recipient. Then, 26.7 mg of cadmium acetate (0.1 mmol) was added following the addition of 5.0 mL of sodium borohydride (25 mM) aqueous solution. Finally, the double phase system reaction was quenched in 15 min. After purification treatment similar to that of the CdS nanoparticles the Au/CdS nanocomposites organic colloid was preserved in refrigerator (277 K) for further analyses.

2.4. Characterization

X-ray diffraction (XRD) patterns were obtained on a Rigaku D/MAX-2200 diffraction using Ni-filtered Cu Kα radiation ($\lambda = 1.5418$ Å). High-resolution transmission electron microscopy (HRTEM) images were performed on a JEOL JSM-2100F TEM with an acceleration voltage at 200 kV. Ultraviolet–visible (UV–vis) absorption spectra were recorded on a Shimadzu UV-3101PC spectrophotometer. Photoluminescence excitation (PLE) and emission (PL) spectra were measured on a Shimadzu RF-5310PC spectrophotometer at room temperature. The quantum yield (QY) of CdS and Au/CdS samples were estimated at room temperature using quinine bisulfate in 1N H_2SO_4 (QY = 0.54) as the reference.

3. Results and discussion

3.1. Structure, composition and size characterization of CdS nanoparticles

Powder XRD pattern of the CdS nanoparticles is shown in Fig. 1. Those peaks of (1 1 1), (2 2 0), (3 1 1), (3 3 1), (4 2 2) and (5 3 1) were clearly observed, which are right consistent with the values of cubic CdS [6,7,13,28]. The peaks were broaden than that of the bulk one, due to their much smaller sizes. HRTEM images and large range selected area electron diffraction (SAED) of the CdS nanoparticles are presented in Fig. 2. It is clearly shown that the CdS were mostly ball-like crystals with an average diameter of about 2–3 nm (Fig. 2(A) and (B)). One can

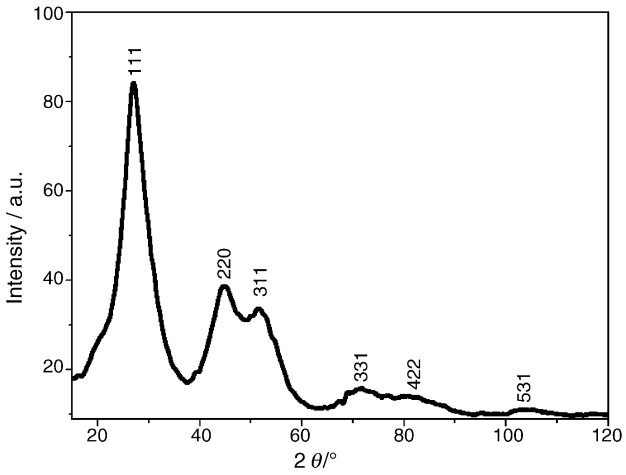

Fig. 1. XRD patterns of CdS nanocrystals.

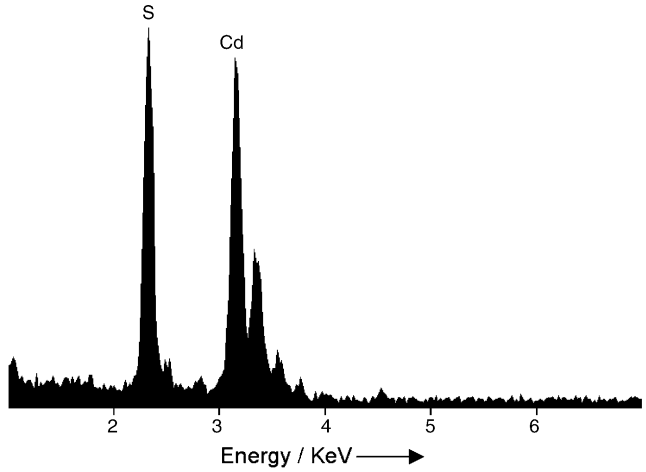

Fig. 3. EDAX of CdS nanocrystals with 49.6 mol% of Cd and 50.4 mol% of S, respectively.

discern that the (1 1 1) lattice spacing of cubic CdS was 0.33 nm, which is in accordance with the XRD result ($d_{111} = 0.32976$ nm). Energy dispersed analysis of X-ray (EDAX) results (Fig. 3) confirms that the composition of those CdS nanocrystals is stoichiometric (Cd = 49.6 mol% and S = 50.4 mol%).

3.2. Sizes adjustment of CdS nanoparticles

When changing the ratio of organic amine surfactant and CdS, aliphatic length of the amines and/or the ultrasound activation time, the CdS nanocrystals size may be adjusted in the nano-size scope. UV–vis absorption spectra were chosen to characterize the sizes of CdS nanocrystals (Fig. 4), based on the following formula, which can be used to calculate the diameters of the nanocrystals when their radii are comparable with the exciton Bohr radius: [49] $E(r) = E_{g(r=\infty)} + h^2/8\mu r^2 - 1.786e^2/4\pi\varepsilon_0\varepsilon_r r - 0.248E_{Ry}$, where the band gap of bulk CdS $E_{g(r=\infty,300\,K)}$ is 2.42 eV, $\mu = 0.17m_0$, $\varepsilon_r = 5.4$, and $E_{Ry} = 29$ meV. A sharp absorption peak at 350 nm with 35 nm of the full width at half maximum (FWHM) in

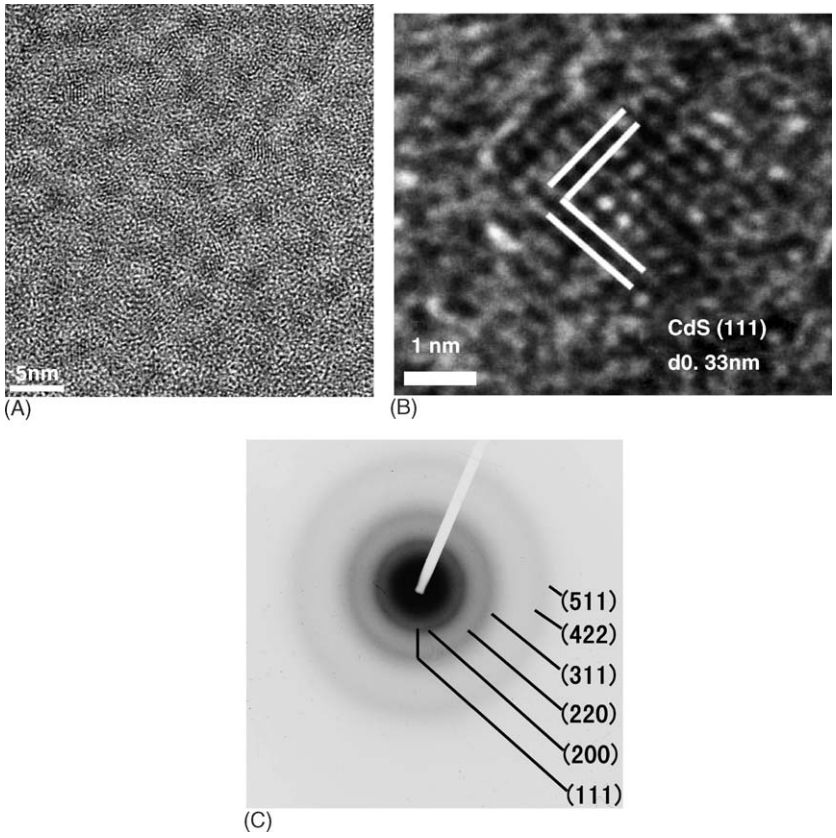

Fig. 2. HRTEM images (A), details of A (B) and SAED (C) patterns of CdS nanocrystals. The bars in (A) and (B) are 5 and 1 nm, respectively.

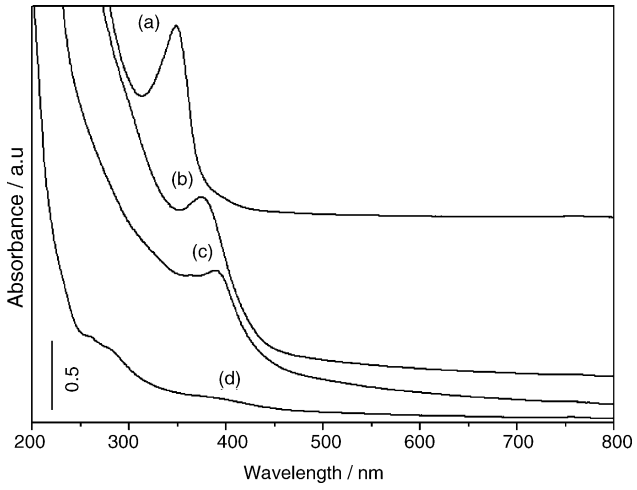

Fig. 4. UV–vis absorption spectra of CdS nanocrystals. Where (a) and (b) correspond to the CdS nanocrystals using octadecyl amine with the amine and CdS molar ratio of 5:1 and the reaction time of 2 and 10 min, respectively; (c) and (d) are related to CdS NC using dodecyl amine and octadecyl amine with the amine and the CdS molar ratios of 5:1 and 1:1, respectively, and the reaction time of 10 min.

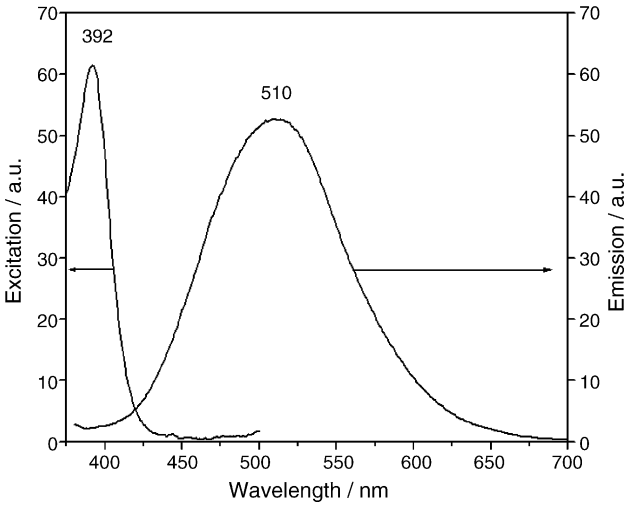

Fig. 5. Photoluminescence excitation and the corresponding emission of CdS nanocrystals with the sizes of 2.6 nm.

correspondence to the calculated dimension of 2.0 nm was observed in Fig. 4(a), when dodecyl amine was used as the surfactant, the reaction time was 2 min, and the molar ratio of amine to CdS was 5:1. Compared with 515 nm that of the bulk CdS crystals, the considerable blue-shift is ascribed to the apparent quantum size effect. Keeping the same molar ratio of amine to CdS, a longer reaction time of 10 min may result in the formation of CdS nanocrystals with a larger dimension of 2.3 nm, which is calculated from the UV–vis absorption at 375 nm (Fig. 4(b)). Further prolonging the reaction time did not helpful for the increase of the sizes. When the dodecyl amine with a shorter carbon chain was used as the surfactant in the reaction system, the CdS nanocrystals with a larger size of 2.6 nm formed, which is related to the absorption peak at 388 nm in Fig. 4(c). The FWHMs of those absorption peaks were about 40 nm, which is due to a little larger crystals size distribution. The less amount of amine may result in formation of the CdS nanocrystals with larger sizes but lower crystallinity. This result is possibly due to the aggregation and growth of the nanoparticles. When the molar ratio of dodecyl amine to CdS was reduced to 1:1, a weak broad absorption peak at about 393 nm (Fig. 4(d)) was observed, which is in accordance with 2.8 nm CdS.

3.3. Optical properties of CdS nanocrystals

PLE and PL spectra of the above typical 2.6 nm CdS nanocrystals are shown in Fig. 5. A green emission peak centered at 510 nm with the QY of about 1.0% was found, which may be attributed to the recombination of the charge carriers within surface states [19,50]. No emission peak at about 600 nm associated with the defects and impurities was observed for those CdS nanocrystals [51,52], which is in correspondence with the high crystallinity and purity. Since the exciton binding energy of CdS is low and small crystals size results in a large amount of surface atoms, the band-edge emission peak was difficult to observe. However, the band–band transition of CdS nanocrystals may be observed on the PLE spectra. The corresponding PLE peak at 392 nm with a narrow FWHM of 21 nm was observed. This result is in consistent with that from the UV–vis spectra, where the band gap absorption was at 388 nm.

3.4. Advantages of this synthetic method and scale-up preparation attempt

Usually, there was a definite separated process at different temperatures between the nucleation and growth stages for most citied traditional preparation of the mono-dispersed nanocrystal colloids. For example, as to the preparation of CdS nanocrystals, a very short time was taken for the nucleation at 573 K to take advantage of the focusing size distribution in the single-phase approach, and then a much long time was needed for the crystal growth at a little low temperature of 523 K [1–4]. Otherwise, the products would be poly-dispersed. The typical reaction occurred at room temperature for our ultrasound activation liquid–liquid two-phase approach, which is much lower than that of the most citied usual preparation method. The reaction procedure may be as follows (Scheme 1): the sodium borohydride was dissolved in water and reacted with Cd(II) source to get active Cd(0) at the water–cyclohexane interface under ultrasound activation. The sulfur source was also activated in the cyclohexane solvent under ultrasonic condition and quickly reacted with the active Cd(0), resulting in the formation of a large amount of nuclei in the first tens of seconds at the water–cyclohexane interface. The nuclei were wrapped by the organic amine surfactants to prevent the aggregation of nuclei at the liquid–liquid interfaces. The wrapped CdS nuclei were automatically dispersed in the whole organic phase. Those nuclei at the liquid–liquid interface could grow up since the reductive sodium borohydride only existed in the aqueous phase, but sulfur and cadmium sources as well as organic amine were in the organic phase. Thus, the formation of CdS nanocrystals was realized through many cycles of diffusion

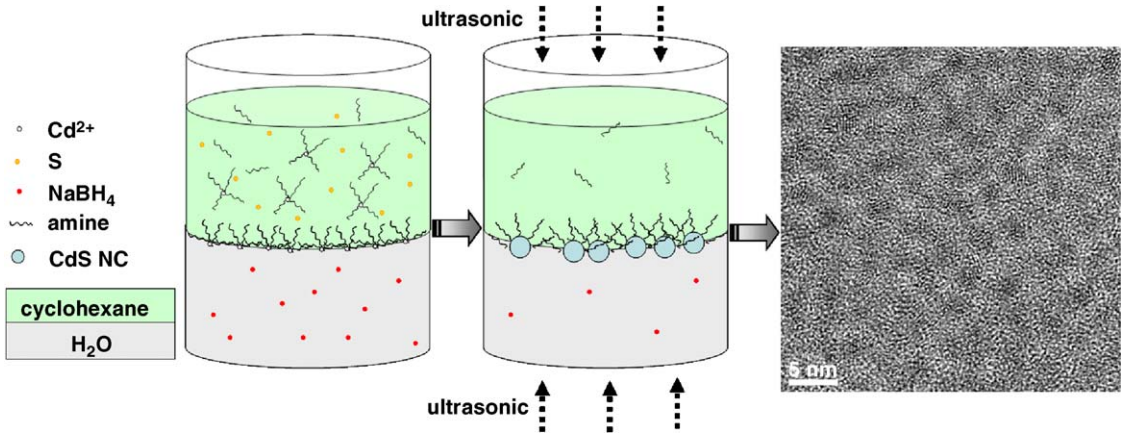

Scheme 1. Synthesis of CdS nanocrystals by a two-phase (water and cyclohexane) approach at room temperature with the assistance of ultrasonic.

of the nuclei to and growth at the interface. The cycles of diffusion and growth model may provide a mild and suitable process for preparation of the nanocrystals. Besides, the reaction time was about 15 min, which is much shorter than that of the most citied usual preparation method.

Since the whole reaction process occurred at room temperature, scale-up synthesis may be realized through simply enlarging the reaction vessels and multiplying the reaction sources. Using 50 times of the related reactants, we have also successfully prepared the CdS nanocrystals with almost the same times of the products, which were in possession of the same dimensions and morphologies. Thus, we believe that the ultrasound activation liquid–liquid two-phase approach has the advantages of fast, energy saving, environmentally benign, high-yield and suitable for scale-up syntheses.

3.5. Expansion studies on bifunctional Au/CdS nanocomposites

The ultrasound activation liquid–liquid two-phase approach for the preparation of binary CdS semiconductor nanocrystal quantum dots may be further expanded to the metal/semiconductor nanocomposites, such as Au/CdS bifunctional nanocomposites. Powder XRD pattern of the Au/CdS nanocomposites is shown in Fig. 6. The peak positions of the composites are right consistent with the values of cubic Au (JCPDS card #04-0784) and CdS. The broaden XRD peaks are due to their small sizes. HRTEM images of Au/CdS (Figs. 7(A) and (B)) showed apparently the heterogeneous structure nanoparticles with the double lattices of Au (1 1 1) and CdS (1 1 1), which are well in correspondence with the XRD results. The diameters of Au cores were around 3 nm and the average particle sizes of Au/CdS composites were about 7 nm based on the TEM analyses. SAED (Fig. 7(C)) showed diffraction rings of both Au and CdS cubic phases, which is in accordance with the results of XRD and TEM.

UV–vis analyses (Fig. 8) show that an absorption peak of the Au/CdS nanocomposites was at 341 nm when they were preserved at room temperature for 10 min. The blue shift of 37 nm compared with 378 nm that of the CdS nanocrystals may be due to the strong influence between Au and CdS bicomponent [49,53]. The diameters of Au cores in our experiments were around 2–5 nm based on the TEM analyses. The average particle sizes of Au/CdS composites were about 6–10 nm. As to the apparent blue-shifts of the absorption peak of CdS occurred for our Au/CdS composites, the possible reason should be that the photo-generated electrons in CdS particles may quickly transfer to the Au nanocrystals, which leads to the strongly quantum size effects. Similar electron transfer phenomena were found for Au or Ag covered titanium dioxide or silicate, etched InP nanowires, and so forth [45–48,54,55]. The typical nanosized Au plasmon band was not observed for the Au/CdS composites, since the particle sizes of some Au cores are near or less than the critical size (2–3 nm) of Au plasmon band bleaching [56]. We speculate that the transferred photo-generated electrons may also cause the surface plasmon absorption of Au to bleach, even though the other particle sizes are a little larger than the critical size, which is accordance to the literature [35,36]. Because of mismatch of the nanocrystals lattices between CdS and Au, the CdS nanocrystals are separated from the Au ones step by step

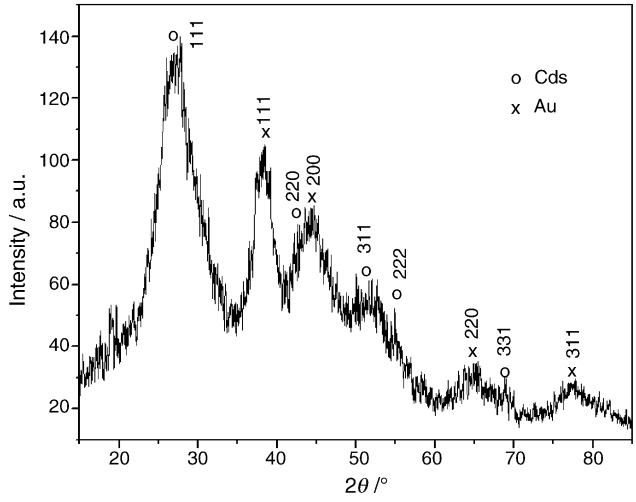

Fig. 6. XRD patterns of Au/CdS nanocomposites.

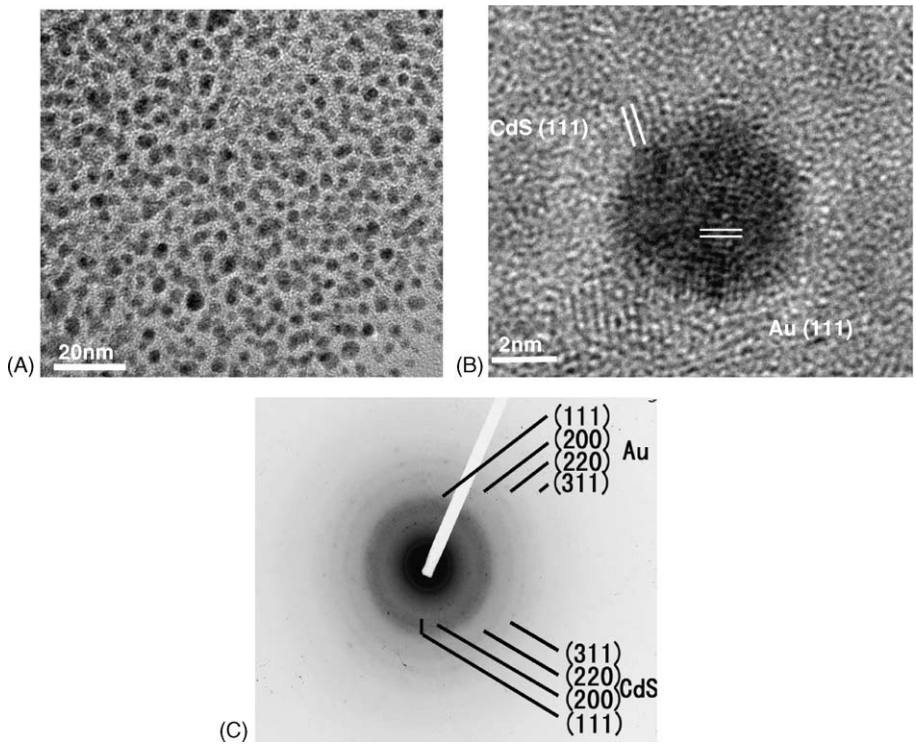

Fig. 7. HRTEM images (A and B) of Au/CdS nanocomposites. SAED patterns (C) of Au/CdS nanocomposites.

and the influence between Au and CdS bicomponents becomes weaker and almost disappear, corresponding to the UV–vis peak position red shift to 375 nm along with the preservation time prolonged to 48 h, which is close to 378 nm that of the CdS nanocrystal single phase. Here, no Au plasmon band was found, which may be due to the rough surface of Au particles with a lot of defects.

Fig. 9 shows the PL peak at 510 nm with the QY listed in Table 1 for the Au/CdS nanocomposites. This peak may be attributed to the recombination of the CdS semiconductor charge carriers within surface states [19,50]. Different from that of the CdS nanocrystal single phase, the PL intensity of the nanocomposites firstly increased along with preservation time and reached a maximum value in 8 h, which is about twice that of the CdS nanocrystal single phase. Then, the PL intensity of Au/CdS nanocomposites decreased. As to

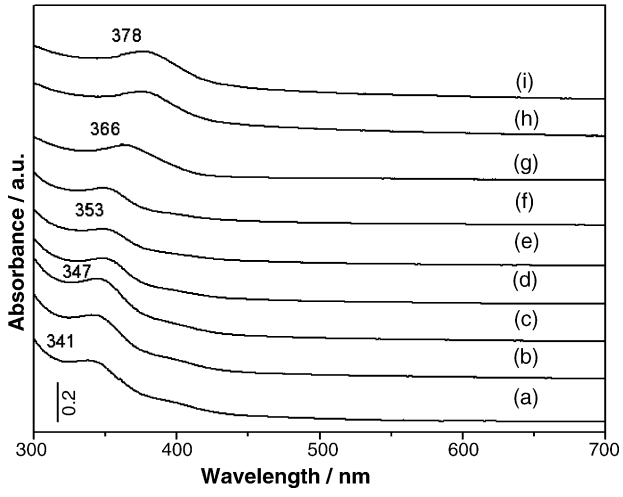

Fig. 8. The absorption spectra of the as-synthesized Au/CdS nanocomposites with the aging times of 10 min (a), 1 h (b), 2 h (c), 4 h (d), 8 h (e), 12 h (f), 24 h (g) and 48 h (h), respectively, compared with CdS nanocrystals prepared under the similar condition with the aging time of 30 min (i).

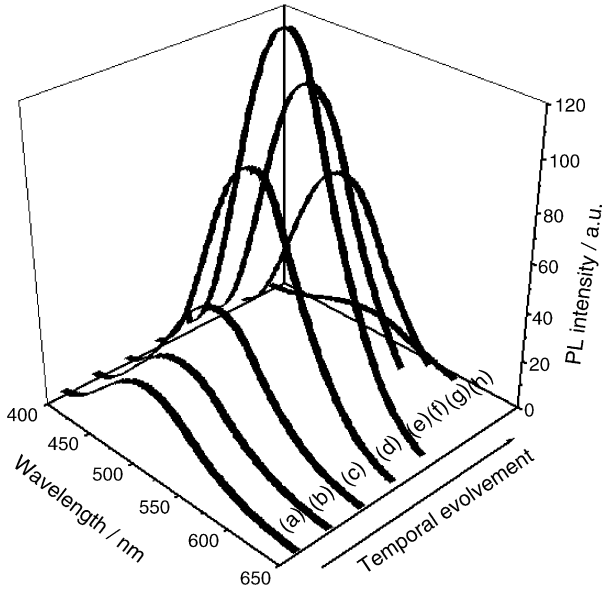

Fig. 9. The photoluminescence (PL) spectra of the as-synthesized Au/CdS nanocomposites with the aging times of 10 min (a), 1 h (b), 2 h (c), 4 h (d), 8 h (e), 12 h (f), 24 h (g) and 48 h (h), respectively.

Table 1
QY of Au/CdS samples at different aging times

t (Aging time)	QY (%)
10 min	0.33
1 h	0.56
2 h	1.1
4 h	1.7
8 h	2.6
12 h	2.1
24 h	1.4
48 h	0.27

the nanocomposite the crystal lattices turn more complex than single-component crystal lattices and many defects produce in the interface between metal and semiconductor. Therefore, there is much nonradiative loss at the earlier stage and the PL intensity of the nanocomposites is even weaker than that of the pure semiconductor. When the preservation time was longer, the effective charge carrier separation occurred for the metal–semiconductor system, more glibly emit phonons were produced in CdS nanocrystals with the increased emission intensity. After that, the metal Au nanoparticles enhanced denature of the CdS nanocrystals possibly similar to the impurity. Further study on the emission mechanism and preparation of stably high intensity nanocomposites luminant are in progress.

4. Conclusion

Combining both ultrasound activation and liquid–liquid two-phase approach brings us a novel approach for the fast synthesis of fluorescent semiconductor nanocrystals at room temperature. The formation may be realized through many cycles of diffusion of the nuclei to and growth at the interface, which provide a mild and suitable process. This fast, energy saving, environmentally benign, high-yield approach could be expanded to the scale-up synthesis of nanocrystals as well as the preparation of metal/semiconductor nanocomposites. This result will benefit greatly to both fundamental mechanism research and industrial utilization development.

Acknowledgement

The authors gratefully thank the financial support by the Creative Foundation (No. SCX200404) of Chinese Academy of Sciences.

References

[1] A.P. Alivisatos, Science 271 (1996) 933.
[2] X.G. Peng, L. Manna, W.D. Yang, I. Wickham, E. Scher, A. Kadavanish, A.P. Alivisatos, Nature 404 (2000) 59.
[3] Z.A. Peng, X.G. Peng, J. Am. Chem. Soc. 123 (2001) 183.
[4] M.W. Yu, X.G. Peng, Angew. Chem. Int. Ed. 41 (2002) 2368.
[5] M. Green, D. Smyth-Boyle, J. Harries, R. Taylor, Chem. Commun. (2005) 4830.
[6] C.B. Murray, D.J. Norris, M.G. Bawendi, J. Am. Chem. Soc. 115 (1993) 8706.
[7] T. Vossmeyer, L. Katsikas, M. Giersig, I.G. Popovic, K. Diesner, A. Chemseddine, A. Eychmuller, H. Weller, J. Phys. Chem. 98 (1994) 7665.
[8] R. Agarwal, C.J. Barrelet, C.M. Lieber, Nanoletter 5 (2005) 917.
[9] Y. Li, E.C.Y. Liu, N. Pickett, P.J. Skabara, S.S. Cummins, S. Ryley, A.J. Sutherland, P. O'Brien, J. Mater. Chem. 15 (2005) 1238.
[10] R. Baron, C.H. Huang, D.M. Bassani, A. Onopriyenko, M. Zayats, I. Willner, Angew. Chem. Int. Ed. 44 (2005) 4010.
[11] I. Tsuji, H. Kato, A. Kudo, Angew. Chem. Int. Ed. 44 (2005) 3565.
[12] M.J. Bruchez, M. Moronne, P. Gin, S. Weiss, A.P. Alivisatos, Science 281 (1998) 2013.
[13] E.D. Sone, S.I. Stupp, J. Am. Chem. Soc. 126 (2004) 12756.
[14] H. Liang, T.E. Angelini, P.V. Braun, G.C.L. Wong, J. Am. Chem. Soc. 126 (2004) 14157.
[15] Y.C. Cao, J.H. Wang, J. Am. Chem. Soc. 126 (2004) 14336.
[16] N.L. Rosi, C.A. Mirkin, Chem. Rev. 105 (2005) 1547, and references therein.
[17] M.C. Daniel, D. Astruc, Chem. Rev. 104 (2004) 293, and references therein.
[18] Y.J. Zhu, W.W. Wang, R.J. Qi, X.L. Hu, Angew. Chem. Int. Ed. 43 (2004) 1410.
[19] W.Z. Wang, I. Germanenko, M.S. El-Shall, Chem. Mater. 7 (2002) 3028.
[20] W.L. Wang, F.L. Bai, Chem. Phys. Chem. 4 (2003) 761.
[21] N.R. Jana, X.G. Peng, J. Am. Chem. Soc. 125 (2003) 14280.
[22] P. Gupta, A. Ulman, S. Fan, A. Korniakov, K. Loos, J. Am. Chem. Soc. 127 (2005) 4.
[23] H. Duan, D. Wang, D.G. Kurth, H.M. Hwald, Angew. Chem. Int. Ed. 43 (2004) 5639.
[24] P.R. Selvakannan, P.S. Kumar, A.S. More, R.D. Shingte, P.P. Wadgaonkar, M. Sastri, Adv. Mater. 16 (2004) 966.
[25] M. Brust, M. Walker, D. Bethell, D.J. Schiffrin, R. Whyman, J. Chem. Soc. Chem. Commun. 7 (1994) 801.
[26] S.L. Horswell, C.J. Kiely, I.A. O'Neil, J. David, D.J. Schiffrin, J. Am. Chem. Soc. 121 (1999) 5573.
[27] S.W. Chen, K. Huang, J.A. Stearns, Chem. Mater. 12 (2000) 540.
[28] D. Pan, S. Jiang, L. An, B. Jiang, Adv. Mater. 16 (2004) 982.
[29] D. Pan, Q. Wang, S. Jiang, X. Ji, L. An, Adv. Mater. 17 (2005) 176.
[30] D.J. Flannigan, K.S. Suslick, Nature 434 (2005) 52.
[31] D. Lohse, Nature 434 (2005) 33.
[32] K.S. Suslick, Ultrasound: Its Chemical, Physical and Biological Effects, VCH, Weinheim, Germany, 1988.
[33] J.J. Zhu, Micronanoelect. Technol. 12 (2002) 21, and references therein.
[34] M. Green, Small 1 (2005) 684, and references therein.
[35] W. Lu, B. Wang, J. Zeng, X.P. Wang, S.Y. Zhang, J.G. Hou, Langmuir 21 (2005) 3684.
[36] P.V. Kamat, B. Shanghavi, J. Phys. Chem. B 101 (1997) 7675.
[37] I. Honma, T. Sano, H. Komiyama, J. Phys. Chem. 97 (1993) 6692.
[38] Y. Lu, Y.D. Yin, Z.Y. Li, Y.N. Xia, Nanoletter 2 (2002) 785.
[39] X.G. Peng, M.C. Schlamp, A.V. Kadavanich, A.P. Alivisatos, J. Am. Chem. Soc. 119 (1997) 7019.
[40] S.U. Son, Y. Jang, J. Park, H.B. Na, H.M. Park, H.J. Yun, J. Lee, T. Hyeon, J. Am. Chem. Soc. 126 (2004) 5026.
[41] X.W. Teng, D. Black, N.J. Watkins, Y.L. Gao, H. Yang, Nanoletter 3 (2003) 261.
[42] H. Zeng, J. Li, Z.L. Wang, J.P. Liu, S.H. Sun, Nanoletter 4 (2004) 187.
[43] H. Gu, R. Zheng, X. Zhang, B. Xu, J. Am. Chem. Soc. 126 (2004) 5664.
[44] H. Kim, M. Achermann, L.P. Balet, J.A. Hollingsworth, V.I. Klimov, J. Am. Chem. Soc. 127 (2005) 544.
[45] T. Hirakawa, P.V. Kamat, J. Am. Chem. Soc. 127 (2005) 3928.
[46] I. Pastoriza-Santos, D.S. Koktysh, A.A. Mamedov, M. Giersig, N.A. Kotov, L.M. Liz-Marzan, Langmuir 16 (2000) 2731.
[47] G. Oldfield, T. Ung, P. Mulvaney, Adv. Mater. 12 (2000) 1519.
[48] K.S. Mayya, D.I. Gittins, F. Caruso, Chem. Mater. 13 (2001) 3833.
[49] L.E. Brus, J. Chem. Phys. 80 (1984) 4403.

[50] Y. Wang, A. Suna, J. Mchagh, J. Chem. Phys. 92 (1990) 6927.
[51] C.J. Barrelet, Y. Wu, D.C. Bell, C.M. Lieber, J. Am. Chem. Soc. 125 (2003) 11498.
[52] D.M. Bagnall, B. Ullrich, H. Sakai, Y. Segawa, J. Cryst. Growth 214 (2000) 1015.
[53] A. Franceschetti, A. Zunger, Phys. Rev. B 62 (2000) R16287.
[54] L.K. van Vugt, S.J. Veen, E.P.A.M. Bakkers, A.L. Roest, D. Vanmaekelbergh, J. Am. Chem. Soc. 127 (2005) 12357.
[55] J. Müller, J.M. Lupton, A.L. Rogach, J. Feldmann, D.V. Talapin, H.J. Weller, Phys. Rev. Lett. 93 (2004) 167402–167411.
[56] M.M. Alvarez, J.T. Khoury, T.G. Schaaff, M.N. Shafigullin, I. Vezmar, R.L. Whetten, J. Phys. Chem. B 101 (1997) 3706.